Available online at www.sciencedirect.com

SciVerse ScienceDirect

Ceramics International 38 (2012) 2835–2843

CERAMICS INTERNATIONAL

www.elsevier.com/locate/ceramint

Effect of powder dispersion on sintering behavior and mechanical properties of nanostructured 3YSZ ceramics

Mamata Pradhan, P.C. Kapur, Pradip *

Tata Research Development and Design Centre (A Division of Tata Consultancy Services Ltd.), 54B, Hadapsar Industrial Estate, Pune 411013, India

Received 25 August 2011; received in revised form 19 November 2011; accepted 21 November 2011
Available online 28 November 2011

Abstract

The aim of this work was to investigate the feasibility of producing dense nanostructured ceramics from commercial zirconia nanopowder by colloidal processing. Our study has demonstrated the adverse effect of the presence of aggregates in the production of nanostructured components. Two techniques were employed to remove aggregates – centrifugation and high energy milling. The finer powder thus produced by centrifugation and/or high energy milling, with an average size of particles around 60–70 nm was consolidated into a green body by a relatively simple low pressure filtration technique (300 kPa). It was possible to prepare green bodies of 47% density with relatively fine and uniform size pores from suspensions containing these powders. The green compacts obtained from finer powder could be sintered to fully dense nanostructured products at a significantly lower temperature (1200 °C) with a soaking period of 0.5 h only with an average grain size of 90 nm only in the sintered compact. In contrast the as received aggregated powder could not be sintered at all to full density even at as high temperature as 1600 °C. The bulk nanostructured 3 mol% yttria stabilized zirconia (3YSZ) compact with an average grain size of 110 nm exhibited Vickers hardness of 12.8 GPa, which is comparable to the available results in the literature.

Keywords: A. Sintering; B. 3YSZ nanoparticles; C. Dispersion; D. High energy milling; E. Nanostructure

1. Introduction

Nanostructured materials have gained importance in functional devices because of special electronic, mechanical and optical properties. For example, nanocrystalline zirconia material used as a smoke detector, ice detector on aircraft wings, engine performance sensor in automobiles [1–4], genosensor to detect *Escherichia coli* [5] in food and water, oxygen sensor in solid electrolyte and as a fuel cell in new-generation energy conversion devices [6]. Because of its transparency in a broad spectral range (visible and UV), allowing application in the optically addressed memory and solar cells [7]. Apart from electronic and optical properties, nanocrystalline zirconia materials have excellent hardness, toughness and thus have tremendous interest in production of fully dense nanostructured zirconia ceramics and investigating their properties [8]. Given the fact, that dry powder processing is associated with inhomogeneity in microstructure, colloidal processing is the preferred route for such functional ceramics [9,10]. Studies on controlling the microstructure and thus mechanical properties of nanostructured polycrystalline zirconia ceramics are of current research interest.

Presence of hard aggregates in nanosize powder is undesirable and requires appropriate means to prevent aggregation during dispersion. In many instances researchers were unable to de-agglomerate the powders in suspension by pH adjustment and/or surface adsorption of polyelectrolyte(s) on the powder surface [11,12]. In case of colloidal processing, achieving high solid loading during dispersion is important for near net shape forming of ceramic components [13–19]. It is generally observed that nanopowders which are dispersed at relatively lower solid loading tend to aggregate with increasing solids concentration in suspensions [20,21].

Prior work in this field, as summarized in Table 1 [11,20–28,30,34–36,45] suggests that it is possible to achieve (even though quite challenging), full densification with minimum grain growth by modifying nano powder synthesis route [22,23,31–33] and/or enhancing the densification kinetics for

* Corresponding author. Tel.: +91 20 6608 6209; fax: +91 20 6608 6399.
E-mail address: pradip.p@tcs.com (Pradip).

0272-8842/$36.00
doi:10.1016/j.ceramint.2011.11.055

Table 1
Literature summary of nano-sized powder processing.

Powder (d_{50}, nm)	Dispersion			Consolidation		Sintering			Reference
	Dispersant	Solid loading (vol.%)	Suspension (d_{50}, nm)	Processes	Green density (%)	Temperature:time (°C:h)	Density (%)	Grain size (nm)	
Y-SZ (15–33)	Dolapix (pH 3)	11	[b]	Dry pressing (600–1000 MPa), slip casting	48 60	1500 (conventional, microwave), two step sintering (1250:0, 1050:20)	97	2150 1300 900	Mazaheri et al. [45]
Pure zirconia (8–13)		[a]		Isostatic (200 MPa)	[b]	Two step sintering (960:10, 1150:2)	99	100–200	Tartaj et al. [36]
Y-SZ (16)	PEI, Dispex A40, TAC	19 and 28	16	Slip cast	55	Two step sintering (1150, 1000:5–10)	99	75	Santacruz et al. [20]
Y-SZ (16)	TMAH + TAC + pH	17	16	Slip cast, die pressed (500 MPa)	54 50	Hybrid microwave/radiant Two step sintering	99.5 99.5	65 70–80	Binner et al. [21]
Alumina (38)	PAA (M.W.: 1800) pH 1.5	40	38	Freeze casting		[b]			Lu et al. [17]
Y-SZ (4)		[a]		CIP (300–1000 MPa)	42–57	1100:4	99.1–99.7	85	Trunec et al. [27]
Y-SZ (25)		[a]	1000	Pressing (280 MPa)	46	1150	>95	150–220	Ghosh et al. [35]
Y-SZ (10–12)		[a]		CIP (300–700 MPa)	[b]	1100:4	87–92	60–80	Maca et al. [26]
Y-SZ (50)	PEI (M.W.: 10,000)	[b]	10,000	Slip casting	[b]	1300:4	98	1000–3000	Duran et al. [11]
Y-SZ (10)		[a]		CIP (300 MPa)		1100	99	80	Maca et al. [25]
Y-SZ (27)	Phosphate ester		[b]	Tape casting	[b]	1350	80	112	Ghosh et al. [34]
Y-SZ (20–40)	Ammonium polycarboxylate (ALON A-6114)	18–20	[b]	Slip casting followed by CIP (400 MPa)	42–49	1150:30	99.5	110	Vasylkiv et al. [23]
Y-SZ (45)	PAA-NH4	25	[b]	Slip cast followed by CIP (400 MPa)	46–52	1150:60	99	95	Vasylkiv et al. [22]
Y-SZ (5)		[a]		Uniaxial pressing (800 MPa)	[b]	950 (air and vacuum)	93 (air) 100 (vacuum)	100 (air) 60 (vacuum)	Srdic et al. [30]
Y-SZ (6)		[a]		Uniaxial pressing (350 Mpa)	43	1000–1070	1000–2	86	Duran et al. [28]
Y-SZ (20)	Polyacrylic acid (M.W.: 2000–3000)	74–85 wt%	[b]	Slip casting	37	1530, 1600:4	98.5	1600	Shan et al. [24]

[a] Dry powder processing of nanoparticles.
[b] Not reported in the literature.

example, by two stage sintering [20,21,36,45], microwave sintering [21], high pressure sintering and spark plasma sintering. The primary objective of the present study is to find a simpler processing route for achieving fully densified nanostructured compact that is, starting with nanopowders, dispersing them effectively followed by low pressure casting so as to achieve fine uniform pore size distribution in the green compact and sintering them at the lowest possible temperature. The mechanical properties of 3YSZ zirconia components thus produced were also determined for comparison.

2. Experimental procedure

2.1. Powder characterization

The morphological feature and size of the particle of the as received 3 mol% yttria stabilized zirconia powder (3YSZ) obtained from Inframat Advanced Materials, USA, were characterized by transmission electron microscopy (TEM). The surface area of the powder was found to be 40 m^2/g as measured by BET (Micromeritics, Flow sorb II 2300). Size distribution of the powder in aqueous suspensions was measured by the conventional laser light scattering technique (Horiba LA-910) with/without dispersant and pH adjustment, after 10 min of ultrasonication. The widely employed transmission electron microscopy (TEM) technique for measuring the size of nanoparticles proved quite inadequate for characterizing nanoparticles in ceramic fabrication. Laser light scattering technique on the other hand provided more reliable estimates of the particle size and helped in characterizing the so called commercial nanopowders for the presence of aggregates.

2.2. Slurry preparation and rheology

Aqueous 3YSZ slurries of solid loading 27 vol.% were prepared with polyelectrolyte dispersants of different molecular weights and sucrose (M.W., 342, Merck). Polyelectrolyte dispersants were sodium polyacrylate (Na-PAA) of molecular weight 15,000 (obtained from Sigma Aldrich) and ammonium polymethacrylate (NH_4-PMA) of molecular weight 10,000–15,000 procured from R.T. Vanderbilt Inc., USA. Unless otherwise mentioned, all slurries were made by planetary ball milling method with zirconox (mixture of zirconia and ceria) media of 10 mm size. The powder to media ratio was maintained at 1:1 by weight. Natural pH of the polyelectrolyte based slurries was measured to be 8–9 and sucrose based slurries were around 6–7 pH. The optimum amount of dispersant was determined by monitoring the shear yield stress of the slurry by vane spindle method using a Brookfield Viscometer, Model DVIII, USA [37]. The vane spindle was rotated at an extremely slow rate of 0.1 rpm and the increase in stress was monitored with time up to 2 min. The amount of maximum stress required to break the particle network in slurries was taken as the shear yield stress of the suspension [38]. Residual coarser aggregates present in the suspension were separated by centrifugation, as needed.

2.3. Consolidation and sintering

Colloidal suspensions containing nanosize zirconia particles were consolidated by applying relatively low pressure of 300 kPa. These experiments were carried out in a highly instrumented and programmable, computer driven laboratory scale pressure consolidation rig, which has been described in detail earlier [39]. Consolidated compacts were dried at room temperature. Organics like polyacrylate and sucrose were removed from the dried samples by heating in steps from 100 °C to 400 °C with 30 °C interval with 30 min soaking at each temperature. After removal of organics, samples were sintered in a Lindberg programmable high temperature furnace (with super kanthal heating elements) as per a predetermined time-temperature sintering cycle. The heating rate was maintained at 5 °C/min. Green and sintered densities of samples were measured using kerosene and water respectively as per ASTM C693. Pore size distributions of green and sintered compacts were measured by mercury porosimetry using a Micromeritics Pore Size Analyzer, Model 9320.

2.4. Microstructures and mechanical properties

Sintered samples were sliced using a diamond cutter and polished using diamond paste of grit size from 6 to 0.25 μm. The polished surface was checked with an optical microscope for scratches and pits and then subjected to thermal etching. All samples were thermally etched at a temperature 100 °C lower than the sintering temperature. The etched samples were examined using scanning electron microscopy. Grain size distribution of the sintered samples was determined by image analyzer software (Image Tool, Version 3.0, University of Texas Health Science Center, San Antonio).

Vickers indentation (ASTM C1327-03) method was used to measure hardness of the sintered samples (Micro hardness tester, Model HM 112, Mitutoyo Corporation, Japan). Hardness of the samples was measured at various loads from 0.1 to 1 kg for dwell time of 15 s. For each sample, ten indentation tests were carried out to obtain average hardness and standard deviation.

3. Results and discussion

3.1. 3.1Characterization of as received particles in suspensions

Commercially available powder supplied by Inframat was observed to be in a highly agglomerated form. The average size (d_{50}) of the powder as measured by TEM was 40 nm (Fig. 1(a)) but was found to be 1640 nm as measured by a laser light scattering technique (Fig. 2). The difference in size distributions as measured by these two different techniques suggested that aggregates were present in the as received powder. Efforts were made to disperse these aggregated powders with different dispersants, pH conditions and milling time. The received powder was de-agglomerated to some extent using three different dispersants (sucrose, Na-PAA and NH_4-PMA) when

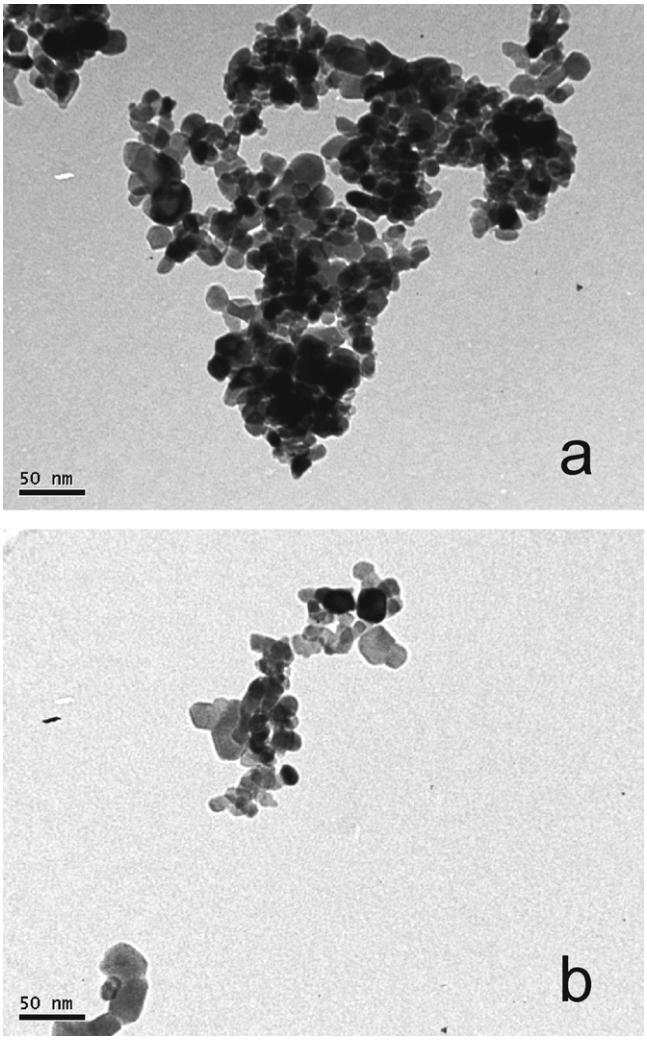

Fig. 1. TEM micrograph of 3YSZ (a) as received aggregated and (b) centrifuged finer powder.

milled in a planetary ball mill for 2 h. As a consequence of attrition milling in planetary mill, the average size of the zirconia powder decreased from 1640 nm to 738 nm due to breakage of aggregates. As compared to polycarboxylates, sucrose was found to be a poor dispersant. The results could not be improved further than what was obtained for milling in a planetary mill in the presence of PMA for 2 h (Fig. 2). Unless otherwise mentioned, the same procedure was followed for dispersion in all subsequent experiments.

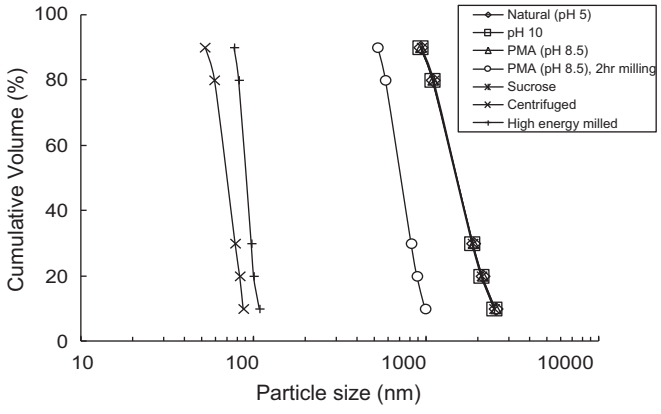

Fig. 2. Cumulative particle size distribution of powder by volume.

The amount of dispersant needed to achieve appropriate dispersion was determined through rheological experiments. Shear yield stress of the concentrated suspension in the presence of dispersants was monitored. The optimum amount of polyelectrolyte dispersant per gram of dry powder was thus found to be in the range of 0.021–0.023 g and the corresponding optimized amount of sucrose dispersant is 0.084 g [40–42]. Yield stress for 27 vol.% solid loading decreased from 8.9 Pa to 4.5 Pa when ammonium salt of polymethacrylate was replaced with sodium salts of polyacrylate. For the same degree of dispersion (same shear yield stress), much higher quantity of sucrose (0.084 g/g of dry powder) was required as compared to Na-PAA and NH_4-PMA. The green compacts were prepared using low pressure filtration set up and were sintered subsequently. The effect of important experimental parameters was systematically studied and the results are discussed in the following section.

Table 2
Sintered densities of compacts from aggregated powder with different dispersants.

Aggregated powder (dispersion and consolidation)					Sintering		
Dispersant	Dispersant/ powder (g)	Solid loading (vol.%)	d_{50} (nm)	Green density (%)	Temperature (°C)	Time (h)	Sintered density (%)
Ammonium salt of polymethacrylic acid	0.023	27	738	41	1200	0.5	83
					1250	2	89
						4	95
					1300	0	89
						0.5	93
						1	94[a]
						2	95
						4	97[b]
					1350	2.5	97
					1400	4	97
Sodium salt of polyacrylic acid	0.021	27	738	41	1200	4	47
					1300	1	49
						4	64
					1600	2	93
Sucrose	0.084	25	1633	41	1200	0.5	82
					1250	2	90
					1300	0	89
						0.5	91
						1	94
						2	94.5
					1350	2.5	97

[a] Average grain size 165 nm.
[b] Average grain size 212 nm

3.2. Choice of dispersant

PMA was found to be the best choice as illustrated in Table 2. The quantity of sucrose required to achieve proper dispersion was as high as 16% by volume (0.084 g/g of dry powder) and therefore it was not pursued further. Between NH_4-PMA and Na-PAA, it was observed that consolidated compacts with comparable green densities could not be sintered to full densification in case of Na-PAA. A temperature as high as 1300 °C with 4 h soaking time was needed to achieve maximum densification for samples consolidated from aggregated suspensions, that is 738 nm size (Table 2). Samples consolidated after dispersion with Na-PAA dispersant attained 65% density only at 1300 °C with a soaking time of 4 h (Table 2). Even after 1600 °C with 2 h soaking, these samples attained 93% densification only. Sodium is known to retard densification as reported earlier in the literature [43].

3.3. Effect of the presence of aggregates on sintering kinetics

Best sintered samples produced from polymethacrylate based slurries, achieved 97% density with an average grain size of 212 nm at 1300 °C with a soaking period of 4 h. Further sintering at higher temperatures (1400 °C) did not lead to higher densification rather it resulted in significant grain growth. To understand the differences in densification, pore size distribution of the green and sintered samples were analyzed through mercury porosimetry. Bimodal pore size distribution was present in all green compacts (Fig. 3). The peak located at 90 nm is most likely due to inter-aggregate voids and the peak at 15 nm may be attributed to intra-agglomerate pores [29]. In sintered compacts, mono-modal distributions of pores were present of size less than 18 nm. During sintering, possibly pores present in green compacts due to intra-agglomerate were

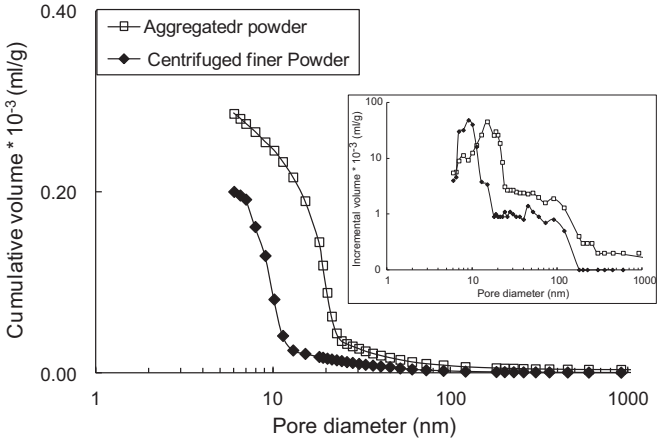

Fig. 3. Pore size distribution of green compacts consolidated from aggregated and centrifuged finer powder.

Table 3
Sintered densities of compacts made from finer powder with ammonium salt of polymethacrylic acid dispersant.

Finer powder (dispersion and consolidation)					Sintering			
Dispersant (ammonium salt of polymethacrylic acid)	Dispersant/ powder (g)	Solid loading (vol.%)	d_{50} (nm)	Green density (%)	Temperature (°C)	Time (h)	Sintered density (%)	Average grain size (nm)
Centrifuged powder	0.023	7	60–70	47	1150	1	94	70
					1200	0.5	100	90
						1	100	85
						4	100	100
					1300	0.5	100	126
						1	100	147
						4	100	155
High energy milled Powder	0.023	10	90	47	1250	1	100	[a]
					1300	4	100	170

[a] Not measured.

eliminated but not the pores due to inter aggregates. Hence, further increase of sintering temperature resulted in relatively coarser inter aggregate pores. The presence of inter aggregate pores in green and sintered compacts was possibly due to the presence of aggregates in the suspension.

In order to confirm the hypothesis that the failure to achieve full densification was possibly due to the presence of aggregates in the optimized suspension, the aggregates were separated by centrifuging 15 vol.% nanozirconia slurry at 10,000 rpm for 15 min. Finer fraction (10 vol.%) thus produced by centrifugation was found to be of an average size of 60–70 nm by laser light scattering (Fig. 2) and 10–40 nm by TEM (Fig. 1(b)).

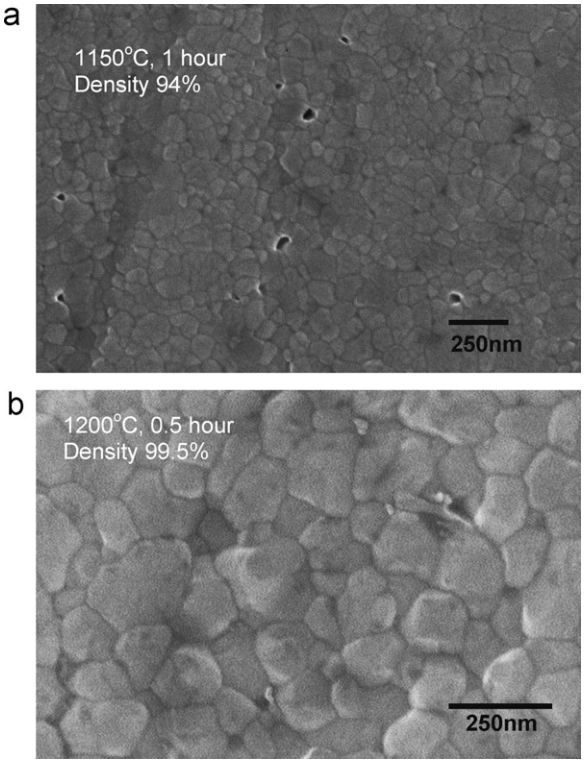

Fig. 4. Nanostructured sintered microstructure of 3YSZ zirconia compacts, from centrifuged finer powder at (a) 1150 °C, 1 h and (b) 1200 °C, 0.5 h of soaking time.

Finer fraction was consolidated in a pressure rig by applying pressures of 300 kPa. The removal of coarser aggregates from the starting powder by centrifugation resulted in an increase in the relative density of green compacts from 41% to 47% by volume. Even though green compacts made with the finer particles had a bimodal pore size distribution (Fig. 3), the peak positions exhibited a marked shift towards smaller size. It seems that the presence of predominantly finer pores in the green compact had a beneficial effect on sintering. As a consequence, these green samples were fully sintered at much lower temperatures, at 1200 °C with a soaking time of 0.5 h only (Table 3). In contrast, the compacts made from coarser powder attained less than 90% relative density under same conditions of sintering (Table 2). Compacts from finer particles were sintered to 94% at 1150 °C with 1 h soaking, with an average grain size of 70 nm (Fig. 4(a)). Further increase in sintering temperature to 1200 °C with a soaking period of 0.5 h showed fully densified compacts with an average grain size of 90 nm (Fig. 4(b)). The corresponding pore size distributions (as measured by mercury porosimetry) of the sintered samples are

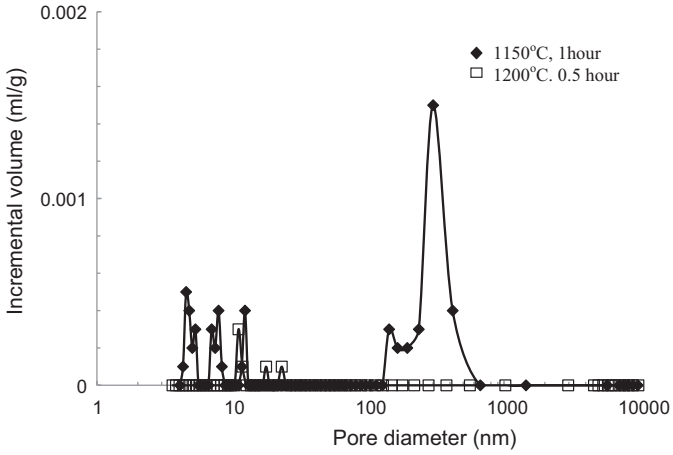

Fig. 5. Evolution of pore size distribution as a function of temperature of 3YSZ green compacts made from centrifuged finer powder.

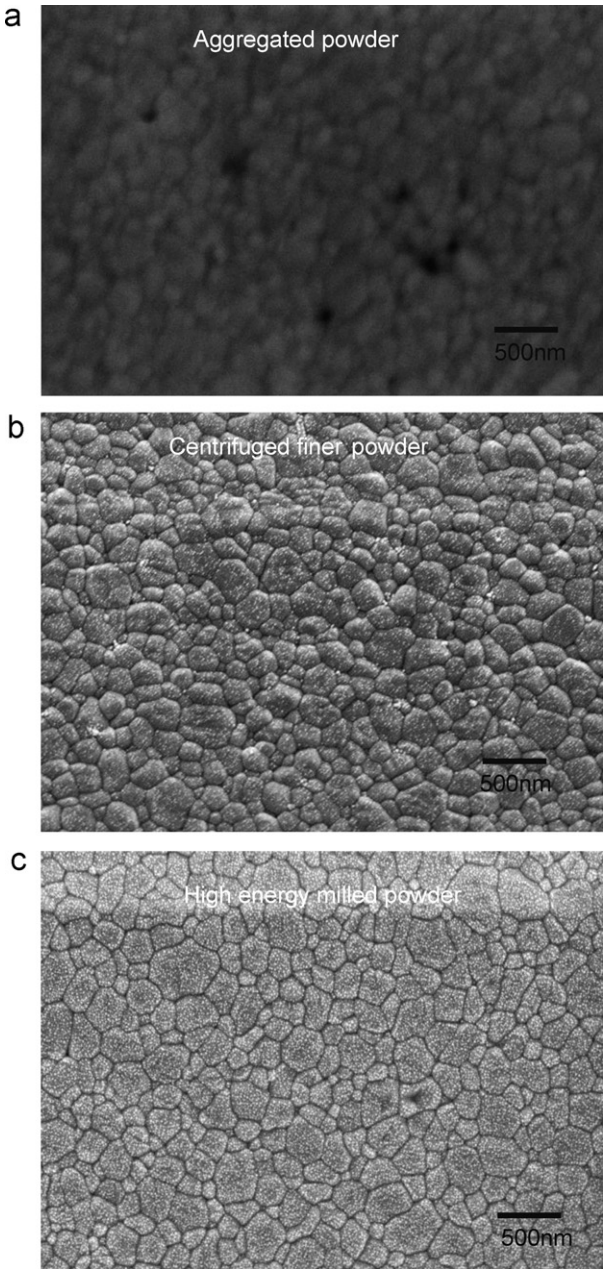

Fig. 6. Sintered microstructure of 3YSZ zirconia compacts from (a) aggregated, (b) centrifuged finer and (c) high energy milled powder at 1300 °C, 4 h of soaking time.

shown in Fig. 5. The major peak at 300 nm observed in case of 1150 °C disappears when sintered at 1200 °C. By varying the sintering temperature from 1200 °C to 1300 °C and hold time from 0.5 h to 4 h, one can achieve full densification with an average grain size in the range of 90–155 nm.

To further validate this hypothesis, as received powder was wet ground for 4 h in a planetary ball mill in the presence of relatively higher dosage of dispersant (20 wt%) and using zirconox media of relatively finer size (2–3 mm) and relatively less powder to media ratio was (1:25) by weight – essentially the grinding conditions were optimized to achieve nanogrinding. After 4 h of grinding, an average particle size of 90 nm (as measured by laser light scattering) was achieved. This powder, labeled as milled powder was consolidated using low pressure filtration technique (300 kPa). Green compacts obtained from this sample of milled powder (90 nm size) could be densified fully at a temperature of 1250 °C with a soaking time of 1 h.

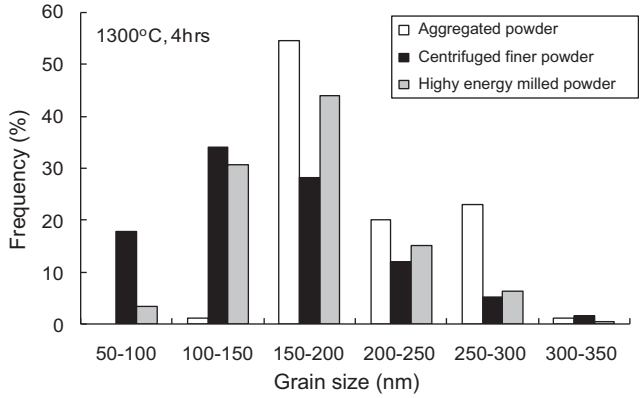

Fig. 7. Grain size distribution of sintered compacts prepared from 3YSZ powder.

It is thus demonstrated that the presence of aggregates adversely affects the sintering phenomena. Removal of aggregates either by centrifugation or by high energy milling results in faster sintering of the compacts leading to full densification at relatively lower temperatures with significantly lower grain growth. We have not conducted detailed experiments to delineate the kinetics of densification as opposed to inadequate sintering at lower temperatures due to the presence of relatively coarser pores in case of sintering of compacts of aggregated powders. It is possible that the sintering kinetics is the same for powders consisting of finer and coarser aggregates but in the latter case bigger pores present in the green compact required higher temperature and longer time to be removed. It is also noteworthy that sintering of finer powders results in attaining more uniform microstructure with finer size grains (Fig. 6). Difference in grain size distribution of sintered compacts obtained from finer and coarse aggregated particles at

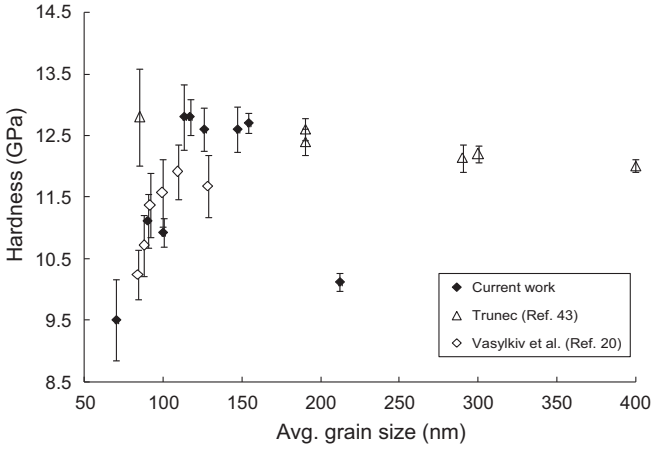

Fig. 8. Vickers hardness of 3YSZ sintered ceramic compacts over a range of grain size.

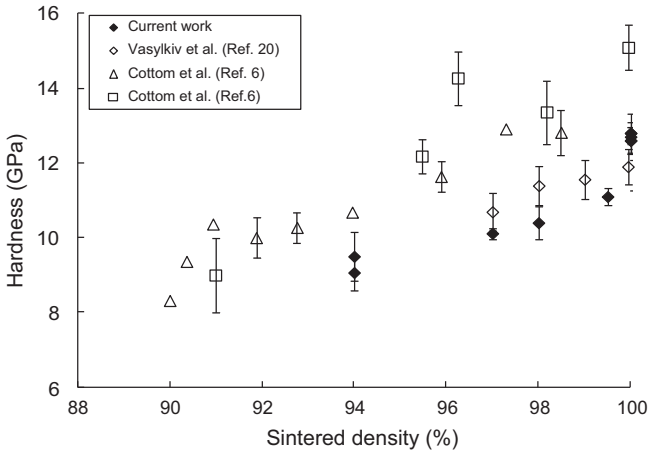

Fig. 9. Vickers hardness of 3YSZ sintered ceramic compacts over a range of density.

1300 °C, with a soaking period of 4 h is illustrated in Fig. 7. In case of coarse aggregated powder there are almost no grains less than 100 nm in the sintered compact (with an average grain size 212 nm) where as the finer powders (produced either by centrifugation or by high energy milling) exhibit grains from 50 nm (average grain size 155 nm).

The corresponding Vickers hardness values for sintered samples as a function of average grain size are summarized in Fig. 8. Our results are comparable with those published in the literature [8,23,44,45]. In the range of 110–150 nm grain size, there is no change in Vickers hardness – an observation consistent with earlier reported data in the literature. Vickers hardness values are plotted as a function of sintered density in Fig. 9. In the present investigation, the hardness values obtained in the range of 9–12.8 GPa are well within the range of reported values [8,23]. Fully dense 3YSZ sintered compact made from finer powder (60–70 nm) thus exhibited hardness values of 12.8 GPa as compared to the hardness (10 GPa) of the most dense compacts (density ∼ 97%) produced from aggregated powder.

4. Conclusions

The presence of aggregates in the so-called nanopowder (3YSZ) zirconia in our case adversely affects the sintering phenomena as well as the final mechanical properties of the sintered compacts. These aggregates can be removed either by centrifugation or by high energy milling optimized to reduce aggregates to nanosizes. Our systematic investigation has shown that the compacts produced from aggregated powders could not be sintered to full density. The maximum possible relative density with these aggregated powders was observed to be 97% with an average grain size of around 212 nm and required sintering at 1300 °C with 4 h of soaking period. Removal of aggregates from the powder by centrifuging and/or grinding helped in achieving highly uniform packing during consolidation with relatively finer pores leading to faster sintering kinetics and enhanced sinterability. It was thus possible to attain full densification at relatively lower temperatures of 1200 °C with a soaking period of 0.5 h only and with an average grain size of 90 nm only. Fully densified 3YSZ ceramics produced from fine nanopowders with no aggregates exhibited the Vickers hardness of 12.8 GPa as compared to a value of 10.8 GPa for those produced from aggregated powders. The need to characterize as received nanopowders through laser light scattering before processing is also demonstrated. TEM studies are not adequate to show the presence of aggregates. It is thus possible to produce nanostructured components of 3YSZ zirconia by conventional colloidal processing and sintering at relatively lower temperatures of around 1200 °C, provided the nanopowders are free of aggregates.

Acknowledgements

The authors would like to acknowledge International Advanced Research Centre (ARCI), Hyderabad, for using their facility (field emission scanning electron microscopy (FESEM) and mercury porosimtery). Authors also wish to acknowledge National Chemical Laboratory (NCL), Pune, for the transmission electron microscopy (TEM) facility.

References

[1] M.N. Rittner, Market analysis of nanostructured materials, Am. Ceram. Soc. Bull. 81 (2002) 33–36.
[2] C. Crab, G. Parkinson, The nanosphere: a brave new world, Chem. Eng. 109 (2002) 27–31.
[3] S.C. Tjong, H. Chen, Nanocrystalline materials and coatings, Mater. Sci. Eng. R. 45 (2004) 1–88.
[4] K. Sobolev, M.F. Gutierrez, How nanotechnology can change the concrete world, Am. Ceram. Soc. Bull. 84 (2005) 15–17.
[5] P.R. Solanki, A. Kaushik, P.M. Chavhan, S.N. Maheshwari, B.D. Malhotra, Nanostructured zirconium oxide based genosensor for *Escherichia coli* detection, Electrochem. Commun. 11 (2009) 2272–2277.
[6] H. Isaacs, ZrO_2 fuel cells and electrolyzers, in: A.H. Heuer, L.W. Hobbs (Eds.), Science and Technology of Zirconia, Advances in Ceramics, vol. 3, American Ceram. Soc., Columbus, OH, 1981, pp. 406–418.
[7] J. Sánchez-González, A. Dıáz-Parralejo, A.L. Ortiz, F. Guiberteau, Determination of optical properties in nanostructured thin films using the Swanepoel method, Appl. Surf. Sci. 252 (2006) 6013–6017.
[8] B.A. Cottom, M.J. Mayo, Fracture toughness of nanocrystalline ZrO_2–3 mol% Y_2O_3 determined by Vickers indentation, Scripta Mater. 34 (1996) 809–814.
[9] F.F. Lange, Powder processing science and technology for increased reliability, J. Am. Ceram. Soc. 72 (1989) 3–15.
[10] J.A. Lewis, Colloidal processing of ceramics, J. Am. Ceram. Soc. 83 (2000) 2341–2359.
[11] C. Duran, Y. Jia, Y. Hotta, K. Sato, K. Watari, Colloidal processing, surface characterization and sintering of nano ZrO_2 powders, J. Mater. Res. 20 (2005) 1348–1355.
[12] S. Jailani, G.V.Franks, T.W. Healy, Potential of nanoparticle suspensions: effect of electrolyte concentration, particle size, and volume fraction, J. Am. Ceram. Soc. 91 (2008) 1141–1147.
[13] C.H. Schilling, M. Sikora, P. Tomasik, C. Li, V. Garcia, Rheology of alumina-nanoparticle suspensions: effects of lower saccharides and sugar alcohols, J. Eur. Ceram. Soc. 22 (2002) 917–921.
[14] N.S. Bell, M.A. Rodriguez, Dispersion properties of an alumina nanopowder using molecular, polyelectrolyte, and steric stabilization, J. Nanosci. Nanotechnol. 4 (2004) 283–290.

[15] A.R. Studart, E. Amstad, M. Antoni, L.J. Gauckler, Rheology of concentrated suspensions containing weakly attractive alumina nanoparticles, J. Am. Ceram. Soc. 89 (2006) 2418–2425.
[16] I. Santacruz, J. Binner, Rheological characterization and coagulation casting of Al_2O_3 – nano zirconia suspensions, J. Am. Ceram. Soc. 91 (2008) 33–40.
[17] K. Lu, C.S. Kessler, R.M. Davis, Optimization of nanoparticle suspension for freeze casting, J. Am. Ceram. Soc. 89 (2006) 2459–2465.
[18] K. Lu, Microstructural evolution of nanoparticle aqueous colloidal suspensions during freeze casting, J. Am. Ceram. Soc. 90 (2007) 3753–3758.
[19] Q. Tan, Z. Zhang, Z. Tang, S. Luo, K. Fang, Influence of polyelectrolyte dispersant on slip preparation of nano-sized tetragonal polycrystals zirconia for aqueous-gel-tape-casting process, Mater. Chem. Phys. 80 (2003) 615–619.
[20] I. Santacruz, K. Anapoorani, J. Binner, Preparation of high solids content nanozirconia suspensions, J. Am. Ceram. Soc. 91 (2008) 398–405.
[21] J. Binner, B. Vaidhyanathan, Processing of bulk nanostructured ceramics, J. Eur. Ceram. Soc. 28 (7) (2008) 1329–1339.
[22] O. Vasylkiv, Y.Sakka, Synthesis and colloidal processing of zirconia nanopowders, J. Am. Ceram. Soc. 84 (2001) 2489–2494.
[23] O. Vasylkiv, Y. Sakka, V.V. Skorokhod, Low temperature processing and mechanical properties of zirconia and zirconia–alumina nanoceramics, J. Am. Ceram. Soc. 86 (2003) 299–304.
[24] H. Shan, Z. Zhang, Slip casting of nanometer sized tetragonal zirconia powder, Br. Ceram. Trans. 95 (1996) 35–38.
[25] K. Maca, M. Trunec, P. Dobask, Bulk zirconia nanoceramics prepared by cold isostatic pressing and pressureless sintering, Rev. Adv. Mater. Sci. 10 (2005) 84–88.
[26] K. Maca, M. Trunec, P. Dobask, J. Svejcar, Sintering of bulk zirconia nanoceramics, Rev. Adv. Mater. Sci. 5 (2003) 183–186.
[27] M. Trunec, K. Maca, Compaction and pressureless sintering of zirconia nanoparticles of ceramics, J. Am. Ceram. Soc. 90 (2007) 2735–2740.
[28] P. Duran, M. Villegas, F. Capel, J.F. Fernandez, C. Moure, Nanostructured and near defect free ceramics by low-temperature pressureless sintering of nanosized Y-TZP powders, J. Mater. Sci. 32 (1997) 4507–4512.
[29] L. Zych, K. Haberko, Filter pressing and sintering of a zirconia nanopowder, J. Eur. Ceram. Soc. 26 (2006) 373–378.
[30] V.V. Srdic, M. Winterer, H. Hahn, Sintering behavior of nanocrystalline zirconia prepared by chemical vapor synthesis, J. Am. Ceram. Soc. 83 (2000) 729–736.
[31] H.B. Qiu, L. Gao, H.C. Qiao, J.K. Guo, D.S. Yan, Nanocrystalline zirconia powder processing through innovative wet-chemical methods, Nanostruct. Mater. 6 (1995) 373–376.
[32] F.C.M. Woudenberg, W.F.C. Sager, J.E. tenElshof, H. Verweij, Nanostructured dense ZrO_2 thin films from nanoparticles obtained by emulsion precipitation, J. Am. Ceram. Soc. 87 (2004) 1430–1435.
[33] Y. Wu, A. Bandyopadhyay, S. Bose, Processing of alumina and zirconia nanopowders and compacts, Mater. Sci. Eng. A 380 (2004) 349–355.
[34] S. Ghosh, A.Guha, A.K. Mukhopadhyay, H.S. Maiti, Sintering and hardness characterization of nanozirconia tapes, Trans. Indian Ceram. Soc. 64 (2005) 213–218.
[35] A. Ghosh, A.K.Suri, B.T.Rao, T.R. Ramamohan, Low-temperature sintering and mechanical property evaluation of nanocrystalline 8 mol% yttria fully stabilized zirconia, J. Am. Ceram. Soc. 90 (2007) 2015–2023.
[36] J. Tartaj, P. Tartaj, Two-stage sintering of nanosize pure zirconia, J. Am. Ceram. Soc. 92 (2009) S103–S106.
[37] N.Q. Dzuy, D.V. Boger, Yield stress measurement for concentrated suspensions, J. Rheol. 27 (1983) 321.
[38] V. Ramakrishnan, Pradip, Yield stress of alumina–zirconia suspensions, J. Am. Ceram. Soc. 71 (1996) 2567–2576.
[39] R.G. de Krester, S.P. Usher, P.J. Scales, D.V. Boger, Rapid filtration measurement of dewatering design and optimization parameters, J. AIChE 47 (2001) 758–1769.
[40] J. Cesarano III, A. Ilhan, Processing of highly concentrate aqueous α-Al_2O_3 slurry stabilized with polyelectrolytes, J. Am. Ceram. Soc. 71 (1988) 1062–1067.
[41] L. Guo, Y. Zhang, N. Uchida, K. Uematsu, Adsorption effects on the rheological properties of aqueous alumina suspensions with polyelectrolyte, J. Am. Ceram. Soc. 81 (1998) 549–556.
[42] J. Cesarano III, A. Ilhan, A. Bleier, Stability of aqueous α-Al_2O_3 slurry with poly (methacrylic acid) polyelectrolyte, J. Am. Ceram. Soc. 71 (1988) 250–255.
[43] J.L. Shi, T.S. Yen, Effect of small amounts of additives on the sintering of high purity Y-TZP, J. Mater. Sci. 32 (1997) 1341–1346.
[44] M. Trunec, Effect of grain size on mechanical properties of 3Y-TZP ceramics, Ceramics – Silikáty 52 (2008) 165–171.
[45] M. Mazaheri, Z.R.Hesabi, F.Golestani-Fard, S. Mollazadeh, S. Jafari, S.K. sadrnezhaad, The effect of conformation method and sintering technique on the densification and grain growth of nanocrystalline 8 mol% yttria-stabilized zirconia, J. Am. Ceram. Soc. 92 (2009) 990–995.